Supporting Information

Characterization of PI/PVDF-TrFE composite nanofiber-based triboelectric nanogenerators depending on types of the electrospinning system

Yeongjun Kim, Xinwei Wu, Chaeeun Lee, and Je Hoon Oh*

Department of Mechanical Engineering and BK21 FOUR ERICA-ACE Center, Hanyang University, Ansan, Gyeonggi-do 15588, Republic of Korea

* Corresponding author (E-mail: jehoon@hanyang.ac.kr)

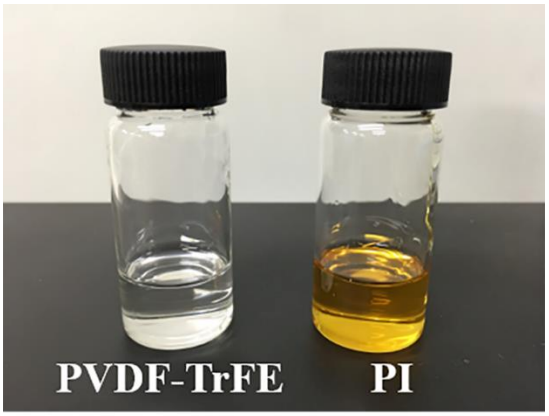

Figure S1. PVDF-TrFE and PI solutions.

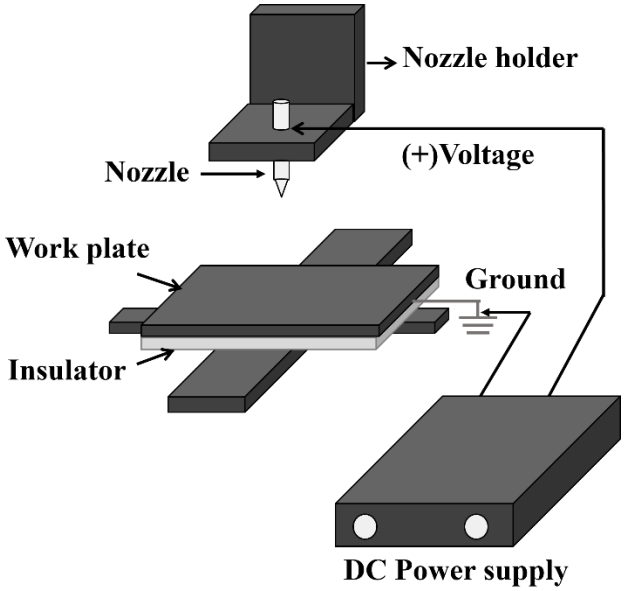

Figure S2. Schematic of an electrospinning system with a plate collector. Note that nozzle could be a single or a conjugated.

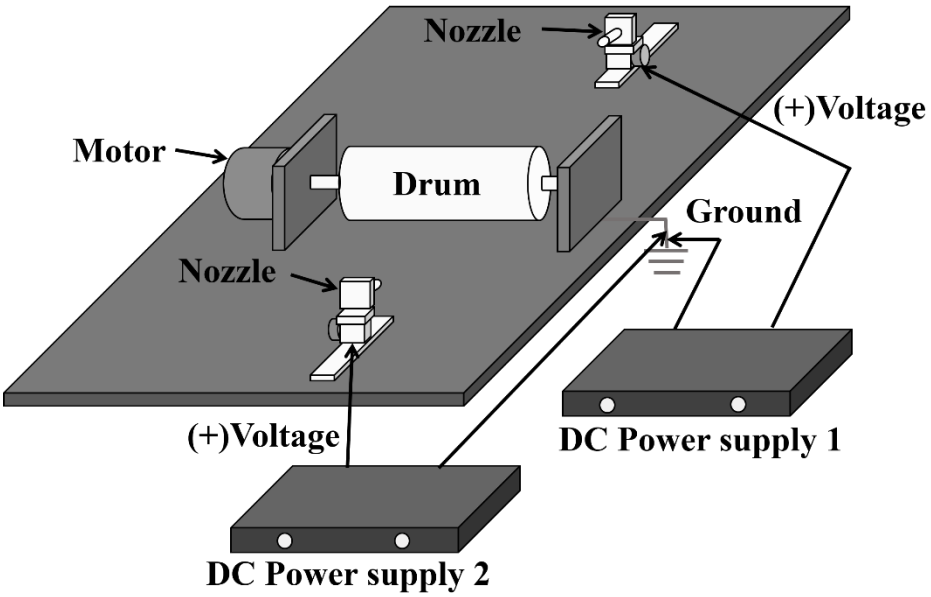

Figure S3. Schematic of an electrospinning system with a drum collector. Note that nozzle configuration could be a single-nozzle, a conjugated-nozzle, or a multi-nozzle.

Figure S4. Image of conjugated-nozzle configuration. The inset image is enlarged view of nozzle tip.

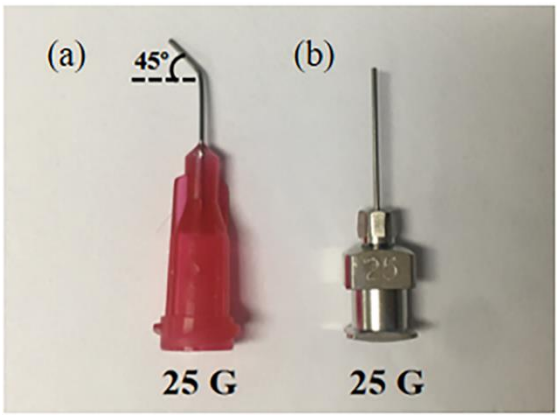

Figure S5. Picture of the nozzles used in (a) the conjugated-nozzle system, and (b) the single-nozzle and multi-nozzle systems.

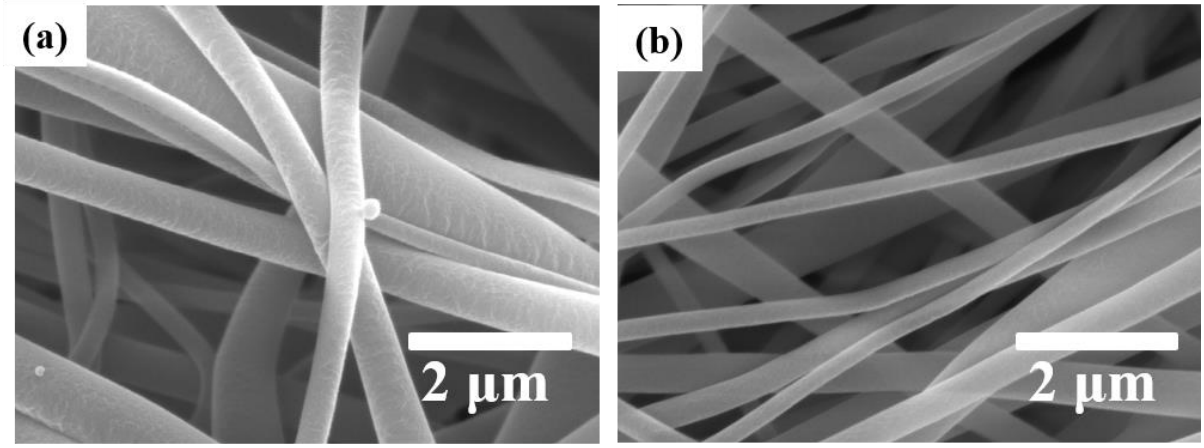

Figure S6. SEM images of (a) PI nanofibers in S1 nanofiber and (b) PVDF-TrFE nanofiber in S2 nanofiber.

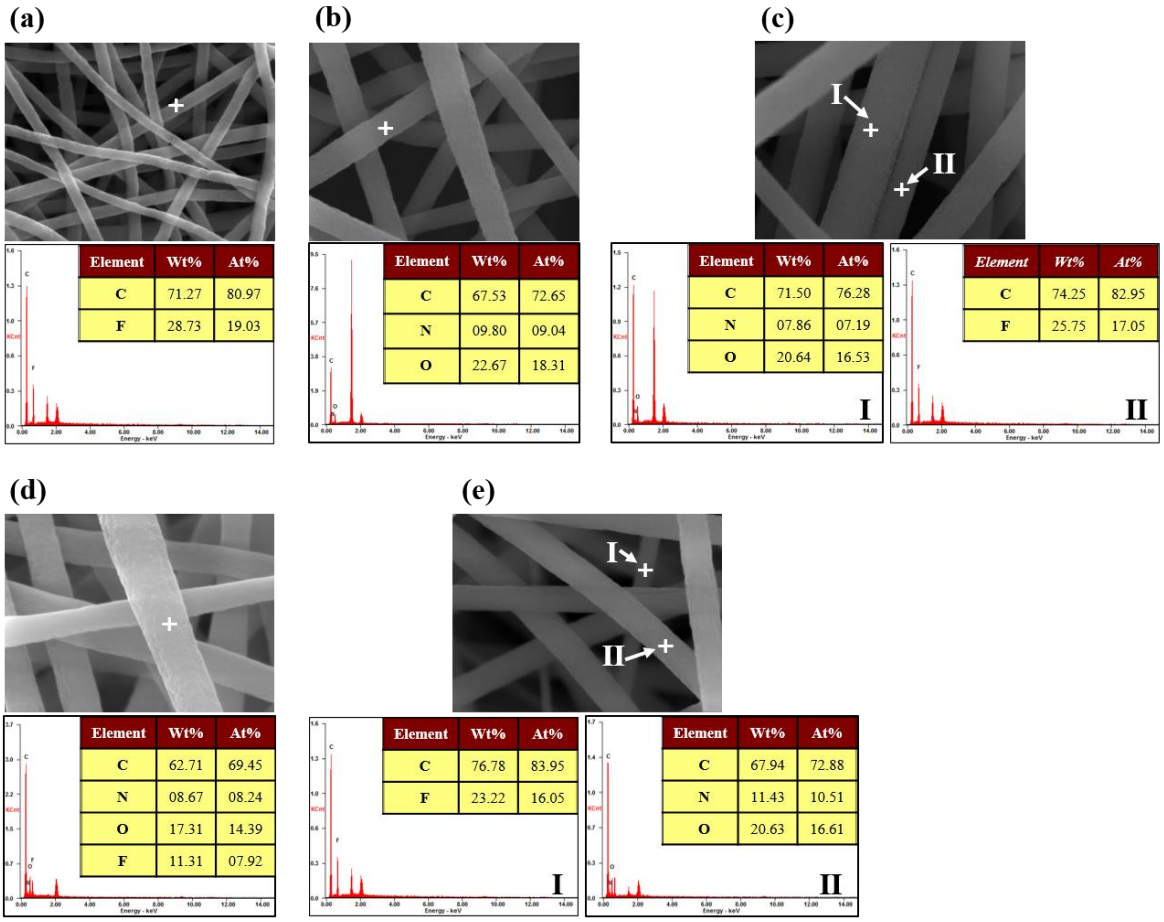

Figure S7. SEM and EDS images of (a) S1 nanofiber, (b) S2 nanofiber, (c and d) C nanofiber, and (e) M nanofiber.

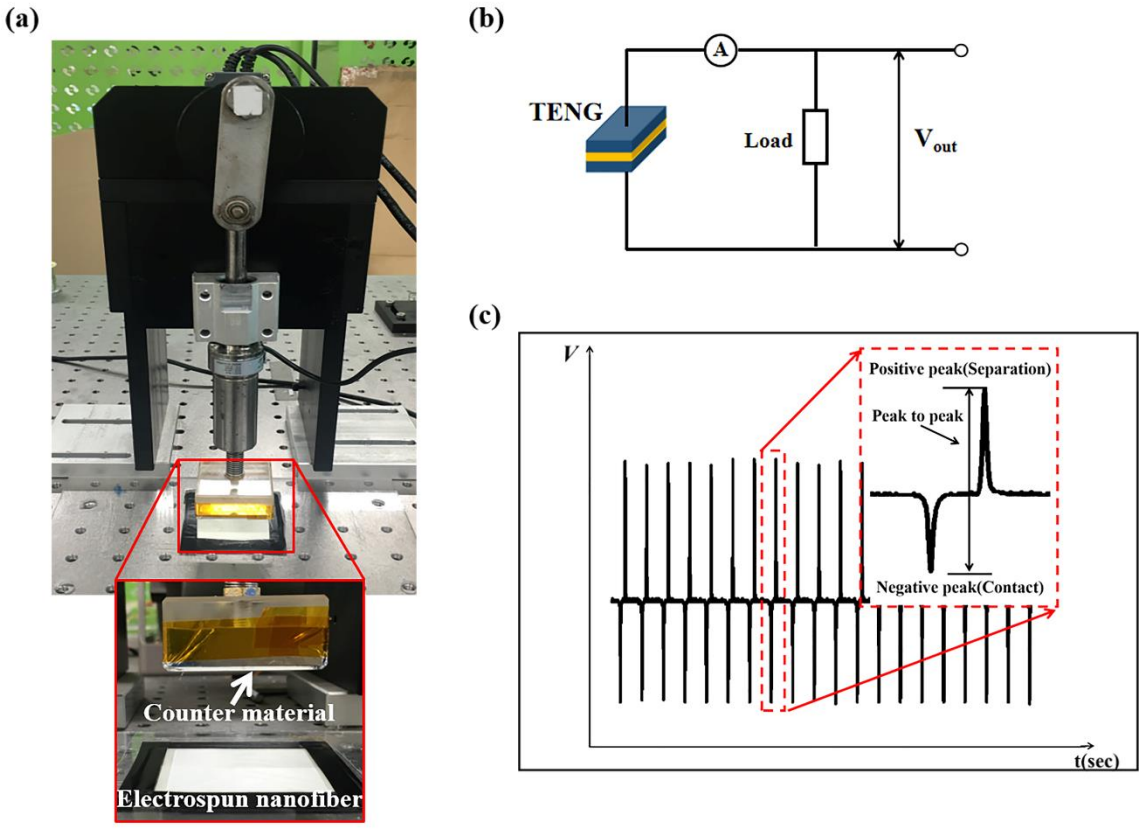

Figure S8. (a) In-house actuating system. (b) Electric circuit for TENG characterization. (c) Output voltage corresponding to the contact and separation between P(VDF-TrFE) nanofibers and a counter material.

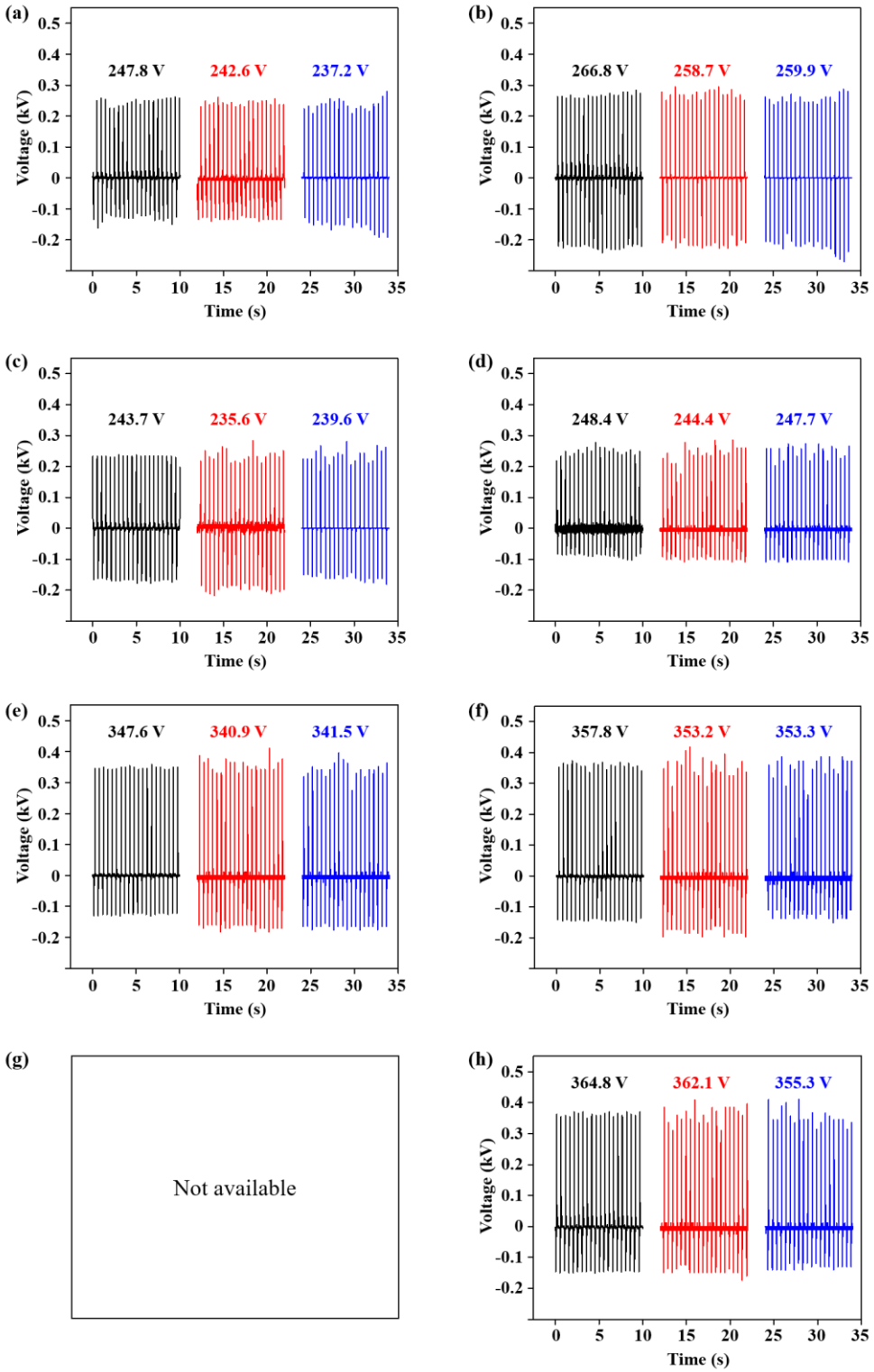

Figure S9. The output voltages of (a) S1_P, (b) S1_D, (c) S2_P, (d) S2_D, (e) C_P, (f) C_D, (g) M_P, and (h) M_D. Note that M_P was not available (see Section 2.2).

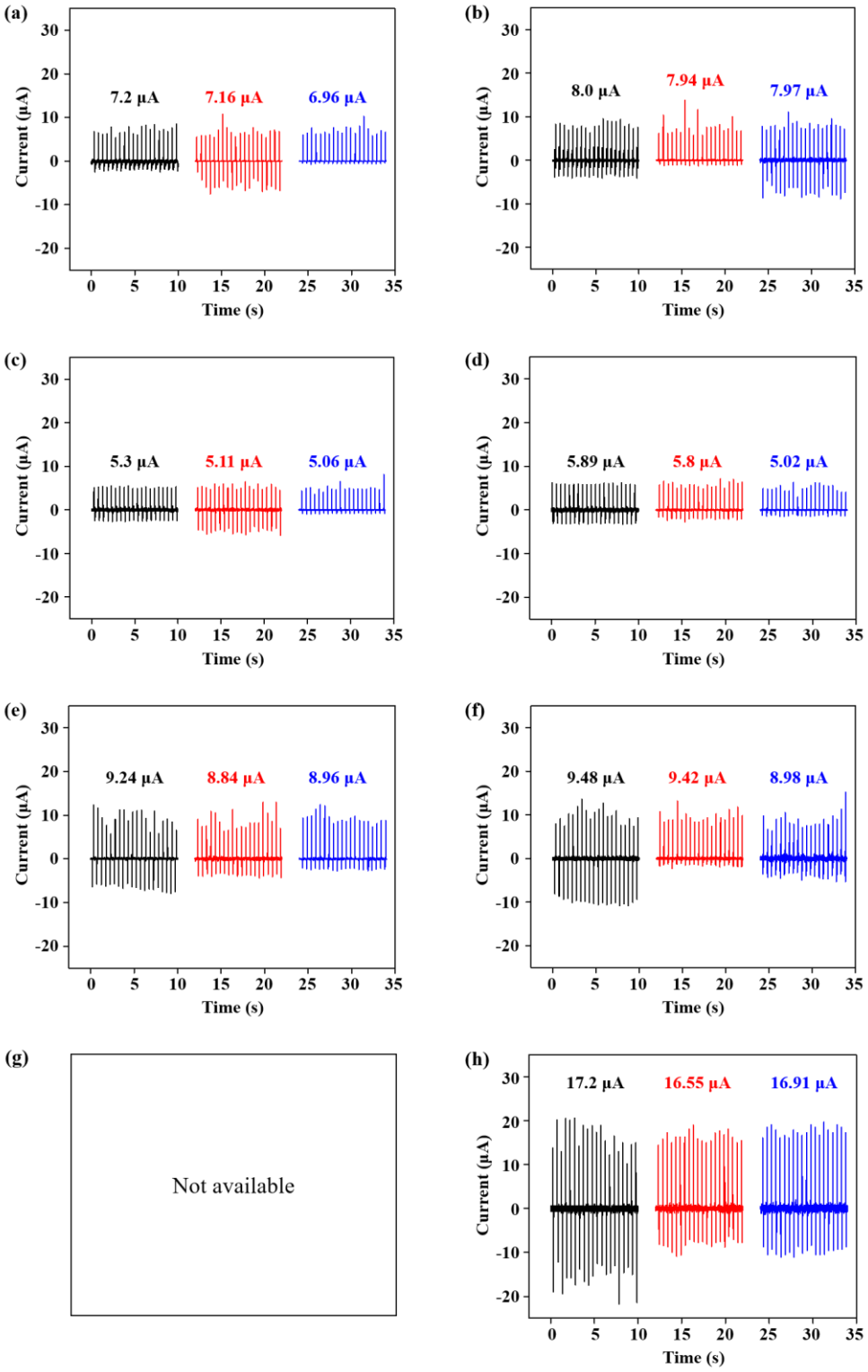

Figure S10. The short circuit currents of (a) S1_P, (b) S1_D, (c) S2_P, (d) S2_D, (e) C_P, (f) C_D, (g) M_P, and (h) M_D. Note that M_P was not available (see Section 2.2).